Scientific Research Publishing

International Journal of Astronomy and Astrophysics, 2024, 14, 120-147
https://www.scirp.org/journal/ijaa
ISSN Online: 2161-4725
ISSN Print: 2161-4717

Refinement of the Proposed Gamma-Ray Burst Time Delay Model

Godson Fortune Abbey[1*], Joseph Simfukwe[1], Prospery Christopher Simpemba[1], Saul Paul Phiri[1], Alok Srivastava[1], Golden Gadzirayi Nyambuya[1,2]

[1]Department of Physic, School of Mathematics and Natural Sciences, The Copperbelt University, Kitwe, Republic of Zambia
[2]Fundamental Theoretical and Research Group, Department of Applied Physics, Faculty of Applied Sciences, National University of Science & Technology, Bulawayo, Republic of Zimbabwe
Email: *godsonabbey88@gmail.com

How to cite this paper: Abbey, G.F., Simfukwe, J., Simpemba, P.C., Phiri, S.P., Srivastava, A. and Nyambuya, G.G. (2024) Refinement of the Proposed Gamma-Ray Burst Time Delay Model. *International Journal of Astronomy and Astrophysics*, **14**, 120-147.
https://doi.org/10.4236/ijaa.2024.142008

Received: May 10, 2024
Accepted: June 25, 2024
Published: June 28, 2024

Abstract

This paper is the second instalment in our study of the observed time delay in the arrival times of radio photons emanating from Gamma Ray Bursts (GRBs). The mundane assumption in contemporary physics as to the cause of these pondersome time delays is that they are a result of the photon being endowed with a *non-zero mass*. While we do not rule out the possibility of a non-zero mass for the photon, our working assumption is that the major cause of these time delays may very well be that these photons are travelling in a rarefied cosmic plasma in which the medium's electrons interact with the electric component of the Photon, thus generating tiny currents that lead to dispersion, hence, a frequency-dependent speed of Light (FDSL). In the present instalment, we "*improve*" on the model presented in the first instalment by dropping the assumption that the resultant pairs of these radio photons leave the shock front simultaneously. The new assumption of a non-simultaneous—*albeit systematic*—emission of these photon pairs allows us to obtain a much more convincing and stronger correlation in the time delay. This new correlation allows us to build a unified model for the four GRBs in our sample using a relative distance correction mechanism. The new unified model allows us to obtain as our most significant result a value for the frequency equivalence of the interstellar medium (ISM)'s conductance $\nu_* \sim 1.500 \pm 0.009$ Hz and also an independent distance measure to the GRBs where we obtain for our four GRB samples an average distance of: ~69.40 ± 0.10, 40.00 ± 0.00, 58.40 ± 0.40, and 86.00 ± 1.00 Mpc, for GRB 030329, 980425, 000418 and 021004 respectively.

Keywords

Gamma-Ray Bursts (GRB), Photon Mass, Plasma, Time Delay, Fireball Model

1. Introduction

One of the most puzzling phenomena in modern astrophysics is perhaps γ-ray bursts (GRBs). These brief flashes of non-thermal γ-ray energy which occur about once a day have consistently defied the *laws of physics* in their explanation. GRBs are highly concentrated high-energy explosions from distant objects deep within space. These explosions create a relativistic blastwave which inevitably collides with the circumburst medium resulting in internal and external shocks [1]. The photons emanating from these GRB shocks possess enormous energies typically of the order of 10^{44} - 10^{47} J [2]-[4] and arrive at Earth as cosmic snipers that are uniformly distributed in the sky [5]. Due to these extreme energies, the prompt emission observed in these GRBs before now was believed to have been generated by a relativistic jet from their central engine [6] [7] [8]. Similarly, an afterglow is likely produced by external shocks from the interaction between the jet material and the circumburst medium [4]. They are believed to be produced by the hottest and most energetic objects in the Universe, such as neutron stars (pulsars) [9], supernova explosions [10], and circumstellar regions of black holes [5].

Despite decades of research, the precise mechanisms driving GRBs and the characteristics of their progenitors remain a subject of intense investigation. However, recent advancements in time delay models [*e.g.*, [11]-[13]] have offered a promising avenue to infer key parameters of these GRBs and the physics of their progenitors. These time delays, resulting from the differential arrival times of photons emitted from different parts of the shock region, encode valuable information about the size and structure of the emitting source. By exploiting the temporal behaviour of GRB's emissions across different frequencies and utilizing theoretical models of light propagation and interaction with the surrounding medium, we can be able to infer the distances to these GRBs using pairs of radio photons emitted in the afterglow stages. A model approach gaining traction involves exploiting the correlations in the time delays observed in the photon as they propagate via the ISM [11].

2. Proposed GRB Time Delay Model

Recently, it has been observed that photons emanating from GRBs and their afterglow experience time delays [14]-[17]. When these time delays are experienced, it causes a change in the frequency of the incoming radiation from the GRB source thereby causing a delay in the arrival time of the photon when detected by the onboard detectors. Time delay is a phenomenon that is well understood in the probing of GRBs [e.g., [3] [18] [19]]. In these supposed time delays, it was observed that Photons emanating from these same GRB events possess different frequencies and also arrive at the telescope at different times [14]-[16].

Unlike most studies on this phenomenon [14] [15] [20]-[25], we do not assume that this time delay is due to the Photon being endowed with a non-zero mass or the usual plasma effect which scales off as ν^{-2}, but that this may very

well be due to the interstellar space being a cold rarefied cosmic plasma, which medium's electrons interact with the electric component of the Photon, thus generating tiny currents that lead to dispersion, hence, a frequency-dependent speed of Light (FDSL) where this speed scales off as ν^{-1}. This FSDL model is a simple, yet profound model derived from the combination of the solutions of the Maxwell-Proca Theory of Electrodynamics (MPED) [26], dispersion and plasma effects. Unlike the time delays due to the *Plasma Effect* and the *Photon Mass Effect* which vary as the square inverse of the frequency *i.e.*: $\Delta t = K\left(\nu_h^{-2} - \nu_l^{-2}\right)$, our new rarefied plasma FDSL model has a time delay dispersion relation that requires the time delay to be proportional to the inverse of the frequency *i.e.*: $\Delta t = K\left(\nu_h^{-1} - \nu_l^{-1}\right)$ thus, making a variation which distinguishes our present FDSL-model from the previously assumed effects [16] [22] [27]. This new variation is of major interest to us and thus forms the basis of our work.

In this model, the theory we came up with was simple and elaborate which is: In Paper I [11], without any exogenous or exotic ideas being brought in, the following dispersion relation was derived directly from Maxwell's four fundamental equations of Electrodynamics:

$$\omega^2 - c_0^2\kappa^2 = -4\omega_*\omega, \tag{1}$$

where: $\omega_* = 2\pi\nu_* = \mu c^2\sigma/4$, $\omega = 2\pi\nu$, with ν being the frequency of the Photon and k its wavenumber. Given that the group velocity ν_g of a wave is given by: $\nu_g = \partial\omega/\partial k$, thus differentiating Equation (1) throughout with respect to k and rearranging, it follows that:

$$\nu_g = \frac{c_0^2}{\omega/\kappa}\frac{1}{2\omega_*/\omega} = \frac{c_0^2}{\nu_p}\frac{1}{1+2\omega_*/\omega} = \frac{c_0^2}{\nu_p}\frac{1}{1+2\nu_*/\nu}, \tag{2}$$

where: $\nu_p = \omega/k$, is the phase velocity. In a vacuum, we have that: $\nu_g = \nu_p = c_0$. This assumption (of: $\nu_g = \nu_p$) was extended to the scenario of a non-vacuum medium and so doing (*i.e.*, maintaining this condition: $\nu_g \neq \nu_p$, in the non-vacuum medium), one obtains:

$$\frac{\nu_g}{c_0} = \frac{1}{\sqrt{1+\dfrac{2\nu_*}{\nu}}}. \tag{3}$$

From Equation (3), it follows that if, D is the distance between the Earth and the GRB, and ν_l and ν_h are the group velocities for the lower and higher frequency Photons, then to first order approximation we have that: $c_0/\nu_g \simeq 1+\nu_*/\nu$, which in turns implies that the time delay Δt, is such that:

$$\Delta t = \frac{D}{\nu_l} - \frac{D}{\nu_h} = \frac{D\nu_*}{c}\left(\frac{1}{\nu_l} - \frac{1}{\nu_h}\right). \tag{4}$$

Thus, if: $\Delta t, D, \nu_l$, and ν_h, are known, the conductance of the interstellar space can be inferred from the value of ν_* since:

$$\sigma = \frac{8\pi\nu_*}{\mu_0 c_0^2} = 8\pi\varepsilon_0\nu_* \tag{5}$$

It is clear that if the laid down theory has any correspondence with physical

and natural reality, then, a plot of $\Delta t \propto \left(\nu_l^{-1} - \nu_h^{-1}\right)$ for the same source (*i.e.*, same D) should-accordingly-yield a straight-line graph with a slope equal to $D\nu_*/c_0$. What Equation (4) implies is that the greater the frequency, the greater the speed for the photon, the meaning of which is that for two photons of different frequencies: ν_h and ν_l such that: $\nu_h > \nu_l$, the time delay will be given by:

$$\Delta t = \frac{D\nu_*}{C}\left(\frac{1}{\nu_l} - \frac{1}{\nu_h}\right). \tag{6}$$

The relation in Equation (6) was applied to the following GRBs: GRB030329, GRB980425, GRB000418 and GRB021004 obtained from [24] and the result was a strong linear correlation between Δt and $\Delta\nu^{-1}$. The obtained linear correlation confirms the theory on which Equation (6) has been derived. Furthermore, in Paper 1 [11], as a major step, Equation (6) assumes that the pair of GRB photons leave the event simultaneously. The above-stated assumption leads to a biased fit wherein the intercept of the graph of Δt vs $\Delta\nu^{-1}$ was made to pass through the point of origin (0, 0) for there to be a zero y-intercept. Despite them giving a good correlation, the four graphs also yield slopes which were used to estimate the conductance of these GRB samples as shown in Paper 1 using Equation (5) with the help of Wright's [28] online cosmological calculator.

In this paper, however, the first argument we made was that the radio GRB photons do not simultaneously leave the GRB event as assumed in the previous paper. The reason for this assumption was to allow us to correct for the difference in the time delay which we confirmed is responsible for the scatter in the first set of graphs we plotted in paper 1 [11] even if they give a good correlation. In line with this assumption, the earlier photon leaves now while the latter leaves a time, t later. We can show that under the above-stated assumption, Equation (6) will be modified to be:

$$\Delta t = \frac{\mathcal{D}\nu_*}{c_0}\left(\frac{1}{\nu_l} - \frac{1}{\nu_h}\right) + t_c, \tag{7}$$

where t_c is a two-fold correction factor we introduced to rectify the time delay in the photon arrival times. Furthermore, t_c is the y-intercept of this unbiased linear regression model and as will become clear in §(5), this t_c will turnout to be the time difference between the emission of the photon pair. This unbiased linear regression model given in Equation (7) can be achieved if the photon pair is to leave the shock front at different times, *i.e.* if these photon pairs are not to leave the shock front simultaneously as is assumed in the biased linear regression model described in Equation (6). Upon pondering, we realise that there is nothing beholding us to this seemingly natural assumption of a simultaneous release of the pairs of these radio photons—*nothing at all*. So, in §(5), we develop the model that does not assume a simultaneous release of these pairs of photons. Rather preemptively, we must say that—this new assumption of a non-simultaneous—*albeit systematic*—emission of these photon pairs allows us to obtain a much more con-

vincing and stronger correlation in the time delay. That is to say, this new correlation allows us to build a unified model of the four GRBs in our present sample wherein, we obtain two major results, mainly:

1) A constant ν_* called the frequency equivalence interstellar medium (ISM)'s conductance which allows us to estimate every other parameter involved with the four GRBs in question.

2) An independent distance measure for the four GRBs samples wherein we obtain the average distance to these four GRBs independent of the redshift as has always been the case.

In the present article, we will present a comprehensive re-analysis of the same four GRBs of Paper 1, whereby we apply the modified time delay model already presented in Equation (7).

Penultimately, we shall give a synopsis of the remainder of the present article. That is to say, §(3) emphasizes the controversy in estimating the distances to GRBs over the years and further provides alternative solutions to this controversy with our model as one of the solutions in resolving this controversy. In §(4), we give a brief overview of the fireball model with special emphasis on how the internal and external shock mechanism of this model give strong support for our ideas on the non-simultaneous release of the photon pairs. §(5) gives a *step-by-step* process of the current time correction methodology we adopted and the constraints imposed on our parameters. Additionally, §(5.1) describe the fitting procedure used to obtain t_c and ν_* respectively. Thereafter, we present our combined analysis and results of the application of the modified time delay model [*i.e.*, Equation (7)] in §(6). §(5.3) presents a description of the data source and the constraints imposed on our sample choice. §(7) summarises our work while §(8) gives a general discussion and the conclusions drawn thereof in the present work.

Lastly and in-closing, we perhaps must hasten and say that, throughout this paper, we assume a flat *Standard* ΛCDM-*Cosmology Model* where we take [29]: $\mathcal{H}_0 = 67.40 \pm 0.50\ \mathrm{km \cdot s^{-1} \cdot Mpc^{-1}}$, $\Omega_\Lambda = 0.685 \pm 0.007$, and $\Omega_m = 0.315$ and that, for all our calculations of the luminosity distances (D_L) to the different GRBs and their host galaxies, we shall use Wright [28]'s online cosmology calculator.

3. Distance Measures

GRBs have been the subject of intense study and debate regarding their distances. Studies such as those by [30]-[32] have delved into the nature of GRBs giving insight into the accurate determination of their distances. If we get our distances wrong in astronomy, astrophysics and cosmology, so is our interpretation of the results thereof—they will be wrong as well. So, the importance of the distance measures that we use to obtain these distances in astronomy, astrophysics and cosmology cannot be overstated. Different distance measures have been used in astronomy, astrophysics and physical cosmology [e.g., [30] [32]-[35]]. These distance measures give a natural notion of the distance between two objects or

events in the Universe. They are often used to tie some observable quantity to another quantity that is not directly observable but is more convenient for calculations such as the comoving coordinates of quasars, galaxy, *etc*. The observable quantities in question are quantities such as the luminosity of a distant star (or GRB, quasar), the redshift of a distant galaxy (or GRB, quasar), or the angular size of the acoustic peaks in the CMB power spectrum. For low redshift objects, these distance measures reduce to the common notion of Euclidean distance. For *e.g.*, the issue of host galaxies and its implications for the distance scale of GRBs by [35], in which they point out the unresolved nature of this distance controversy. Furthermore, they emphasized the importance of low-redshift GRBs in anchoring primary distance indicators, highlighting the challenges posed by the scarcity of such events.

In these aforementioned cosmological methods, two models have always stood out as the major determining factors of the distances to GRBs. They are: the *angular size redshift method* ($\mathcal{D}_A$) [36]-[40] and the *luminosity distance method* ($\mathcal{D}_L$) [40]-[45]. The angular size redshift method offers a promising avenue for estimating the distances of GRBs by leveraging redshift data and angular size measurements, while the luminosity distance $\mathcal{D}_L$ is the Light-travel distance or the look-back time ($t = \mathcal{D}/c_0$) and can be typically calculated [see e.g. [46]-[49]] by assuming a Friedman Universe—*i.e.*, the expanding Universe within the framework of the standard Cosmological-Constant Cold-Dark-Matter model (ΛCDM-model); and that the redshift z is solely due to the expansion of the Universe.

In conclusion, while strong evidence supports GRBs' cosmological distances, the field continues to grapple with uncertainties and the need for further observations to refine distance measurements and enhance our understanding of these intense astrophysical phenomena. In the sub-section following, we shall briefly discuss the methods adopted to resolve these controversies and see how our model plays a major role in advancing GRB distance estimation. Of particular interest in our present expedition are the luminosity (d_L)and Light travel distances (d_{LT}).

3.1. Luminosity Distance

Let, $F(d_L)$, be the flux received at the radial distance, d_L, away from a Light source of luminosity, *L*. This distance, d_L, is known as the luminosity distance. From the inverse square law that describes the spread of the flux from the source, we know that:

$$F(d_L) = \frac{L}{4\pi d_L^2}, \tag{8}$$

so that:

$$d_L = \sqrt{\frac{L}{4\pi F(d_L)}}, \tag{9}$$

This luminosity-distance relation applies in the case of photons propagating

in free space (*i.e., vacuo*) whose refractive index, n_r, is identically equal to unity: $n_r \equiv 1$. In the case of a non-*vacuo* medium, there will be extinction caused by a nonzero optical depth, τ, of the Interstellar Medium (ISM) due to the intervening material in the spaces along the path of the photons reaching our telescopes from the given source. In this case, the flux is now given by:

$$F\left(d_L\right)=\left(\frac{L}{4\pi d_L^2}\right)\mathrm{e}^{-\tau}=\frac{L}{4\pi d_L^{2\tau}}, \tag{10}$$

where we have written:

$$d_{L^\tau}=\mathrm{e}^{\tau/2}d_L, \tag{11}$$

and we shall call this distance, d_{L^τ}, the extinction corrected distance. Apart from the luminosity distance, we can also measure the physical distance to the source *via* what is known as the Light travel distance and we shall give an exposition of this in the next subsection.

3.2. Light Travel Distance

Herein denoted by the symbol d_{LT}, the *Light Travel Distance*, is a cosmological concept that refers to the distance Light travels from one point (A) to the other (B), in particular, the distance Light could travel say from one galaxy to our own telescope at the time of observation. The Light travel distance can be important for understanding phenomenon such as the age of the Universe, its expansion rate and the spatial size of the observable Universe for example. Wholly within the framework of Einstein [50]-[52]'s General Theory of Relativity (GTR), the Light travel distance is calculated with respect to proper time $\mathrm{d}t$, *i.e.*:

$$d_{LT}=\int_0^{\tau_r}c_0\mathrm{d}t. \tag{12}$$

From the homogeneous and isotropic metric tensor of Friedman [53], Lemaître [54], Robertson [55]-[57] and Walker [58] (FLRW-metric), which is the fundamental metric that defines the ΛCDM cosmology model—by setting the proper time in this metric to equal zero for the propagation of Light in an FLRW-Universe—one can show from it that, the Light travel distance, d_{LT}, defined in Equation (12), is such that:

$$d_{LT}=d_{\mathrm{H}}\int_0^z\frac{\mathrm{d}z}{\left(1+z_\lambda\right)\sqrt{\Omega}}=d_{\mathrm{H}}f\left(z_\lambda\right), \tag{13}$$

where off cause:

$$f\left(z_\lambda\right)=\int_0^{z_\lambda}\frac{\mathrm{d}z_\lambda}{\left(1+z_\lambda\right)\sqrt{\Omega}}, \tag{14}$$

and: $d_{\mathrm{H}}=c_0/\mathscr{H}_0$, is what is called the Hubble distance—with:

$$\Omega=\frac{1}{\mathscr{H}_0^2}\frac{\dot{\mathfrak{a}}^2}{\mathfrak{a}^2}=\Omega_{\mathrm{m}}+\Omega_\Lambda+\Omega_k. \tag{15}$$

The Ω's appearing in Equation (15) are the usual Ω-parameters used in cos-

mology—with, Ω, being the total Ω-parameter; while, Ω_{m}, is the Ω-matter parameter; Ω_{Λ}, is the Ω-vacuum parameter for the Λ-cosmological field; and, Ω_k is the Ω-curvature parameter and the *a* is the scale factor describing the expansion of spacetime in the Ω_{m} cosmology model and, $\mathscr{H}_0$, is the Hubble-Lemaître constant [59] [60].

The above defined Light travel distance is for the case of free space. In a non-*vacuo* medium, the refractive index comes into because the speed of Light is no longer, c_0, but, c_0/n_r, where, n_r, is the refractive index. Since the refractive index is a function of the wavelength of the emitted and this wavelength is itself a function of the redshift, it follows that: $n_r = n_r(z_\lambda)$, and all this leads to the following, refractive index corrected Light travel distance:

$$d_{LT}^{n_r} = \int_0^{\tau_r}\left(\frac{c_0}{n_r}\right)\mathrm{d}t = d_{\mathrm{H}}\int_0^z \frac{\mathrm{d}z}{n_r(z_\lambda)(1+z_\lambda)\sqrt{\Omega}}. \tag{16}$$

3.3. Synthesis

From the above, we have defined the luminosity $\left(d_L, d_{L^\tau}\right)$ and Light travel $\left(d_{LT}, d_{LT}^{n_r}\right)$ distances. From this exposition, it is clear that in the even of Light traveling in a *vacuo*, the luminosity distance must equal to the Light travel distance—*i.e.*: $d_L = d_{LT}$. In the non-*vacuo* medium, the same must be true—that the extinction corrected luminosity (d_{L^τ}) must equal to the refractive index corrected Light travel distance—*i.e.*: $d_{L^\tau} = d_{LT}^{n_r}$. Written explicitly in-terms of, d_{LT}, we have that:

$$d_{LT}^{n_r} = \mathrm{e}^{\tau/2} d_{LT}. \tag{17}$$

The attenuation effects due the non-*vacuo* nature of the ISM do not affect the redshift. What this means is that the redshift derived Light travel distance, d_{LT}, is the true measure of the distance to our GRB source—*i.e.*, $D = d_{LT}$, hence:

$$D = \mathrm{e}^{-\tau/2} d_{LT}^{n_r}. \tag{18}$$

So, we shall herein distinguish between luminosity distance and Light travel distance.

4. Fireball Model

As is widely known, a highly effective framework for interpreting observations of GRBs has been made available in the form of the fireball model [61]-[64]. The fireball model is commonly employed to explain the mechanism that produces the radiation we detect from most GRBs. The most widely accepted, and almost certain explanation for GRB production according to the fireball model is that when there is an ejection of extremely high energetic jets due to the merger of two neutron stars (NS-NS) or a neutron star and a black hole (NS-BH) as depicted in **Figure 1**, the enormous release of energy gives rise to a Poynting-flux-dominated Magneto-hydrodynamics (MHD) wind with a luminosity of approximately 10^{50} erg·s^{-1} [65] within the ISM confined to the jet cone.

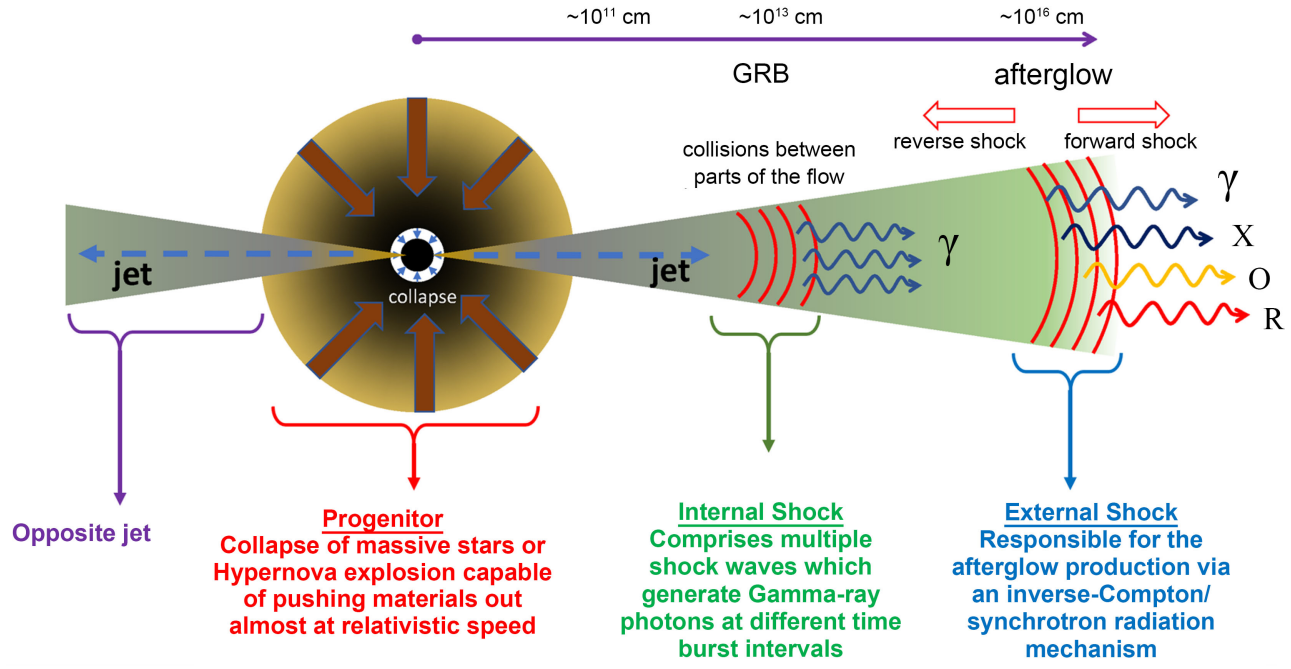

Figure 1. A modified cartoon depiction showing schematics of the fireball model and the basic components of the internal and external shocks [72].

To describe both the initial burst of γ-rays and the lengthy afterglow, the fireball model employs two separate shock wave models—namely, the *internal and external shock wave models* [66] [67]. As depicted in **Figure 1**, internal shocks are responsible for the highly energetic γ-ray particles, while external shocks are predominantly thermal emissions produced as the energy transferred from the shock waves is deposited into the interstellar medium (ISM). The resulting broadband synchrotron radiation evolves as the external shock propagates outward into the surrounding medium, depending on various fundamental characteristics of the explosion, the specifics of the internal shock evolution, and the density profile of the medium into which it expands [68] [69]. When shocks from this external surrounding circumburst matter delay this flow of electrons, the afterglow appears with varying frequencies ranging from X-ray to optical wavelengths [70]

So far, Little is known about the physics of relativistic shocks, the mechanism of the shock acceleration, and the methods for boosting magnetic fields to the necessary magnitudes to generate the observed synchrotron emission we detected from the fireball [67] [71]. Further uncertainties stem from the fact that the circumburst medium's structure and outflow shape are unknown and may very well have an intricate nature. It is on the premise of these uncertainties that we anchor our modified emission model where-in we now have the radio photon pairs not simultaneously leaving the GRB event as has been assumed in Paper (I) [11]. We aim to show that under the above-stated new assumption of non-simultaneous emission of the radio photon pair, the time delay experienced by these photons may very well be a result of the series of shock waves generated

by the internal and external production mechanism. This may also lead us to understand the shock dynamics and/or the spatial sizes (ΔD) of the shocks. We believe that under the current fireball model, the GRBs will be delayed by a fraction of the difference between the spatial sizes obtained from our calculation. Due to the scope of this current instalment, we will limit our result to the average distance (D_{avg}) and conductance of the ISM. The spatial size (ΔD) and the expected outcome of the internal and external shock dynamics will be discussed extensively in the next instalment.

5. Non-Simultaneous Photon Emission Model

As stated in the introductory section—the assumption that the low (ν_l) and high (ν_h) frequency photons are released simultaneously is to be done away with because it is very much possible that the low (or perhaps the high) frequency photon is released first, with the high (low) frequency photon is released a time t_c later (or *vice-versa*). In this event, the photon travel times t_l and t_h of the low and high frequency photons, respectively—will be related as follows:

$$t_l = \frac{D}{\nu_l} + t_c, \tag{19}$$

$$t_h = \frac{D}{\nu_h}, \tag{20}$$

where, likewise: ν_l and ν_h are the speed of the low and high-frequency photons, respectively. From the foregoing, it follows from Equation (5), that:

$$\Delta t = t_l - t_h = \frac{D}{\nu_l} - \frac{D}{\nu_h} + t_c. \tag{21}$$

As given in Paper (I), if we are to substitute into Equation (21), the following:

$$\frac{1}{\nu_l} = \frac{1}{c_0}\left(1 + \frac{\nu_*}{\nu_l}\right), \tag{22}$$

$$\frac{1}{\nu_h} = \frac{1}{c_0}\left(1 + \frac{\nu_*}{\nu_h}\right), \tag{23}$$

then, one will be led to Equation (6). In this way—as promised, we have justified Equation (7).

It is important to note that if t_c is a random variable—*the meaning of which is that this time is not the same for each photon pair*—it would give rise to a clearly visible scatter in the data points along some imagined average straight line. If t_c is uniform for all the data points—imply some welcome define and systematic origin, then, the resulting data points—*if plotted in an unbiased*[1] *manner*—they would lie on a straight line that does not pass through the (0, 0)-point of origin as is the case with the data point of the GRBs in our sample. In the next section, we will describe the procedure that we employed in order to

[1]By "unbiased plot", we mean a plot that not force the linear graph to pass through the (0, 0)-point of origin as has been done on Paper (I).

calculate t_c and ν_*.

5.1. Fitting Procedures

As promised above, we here describe [in §(5.1.1) & (5.1.1)] the fitting procedures employed to arrive at a value for the time delay correction t_c, the value of the frequency equivalent of the ISM's conductance ν_* and the average distances to the GRBs. The complete data employed and the combined results for these procedures are outlined in Table A5.

Time Delay Correction (t_c)

To obtain t_c, the following procedures were carried out:

1) First, we isolated the different subgroups of the individual GRBs. That is to say, we noted that for each GRB source, there exist two distinct subgroups—were for:

a) GRB 030329, as can be seen in the left panel of **Figure 2**, we have (*a*, *b*, *c*, *d*, *e*, *f*, *l*, *m*, *n*, *o*) and (*g*, *h*, *i*, *j*) data points forming the two subgroups with GRB 0302329k being an outlier data point.

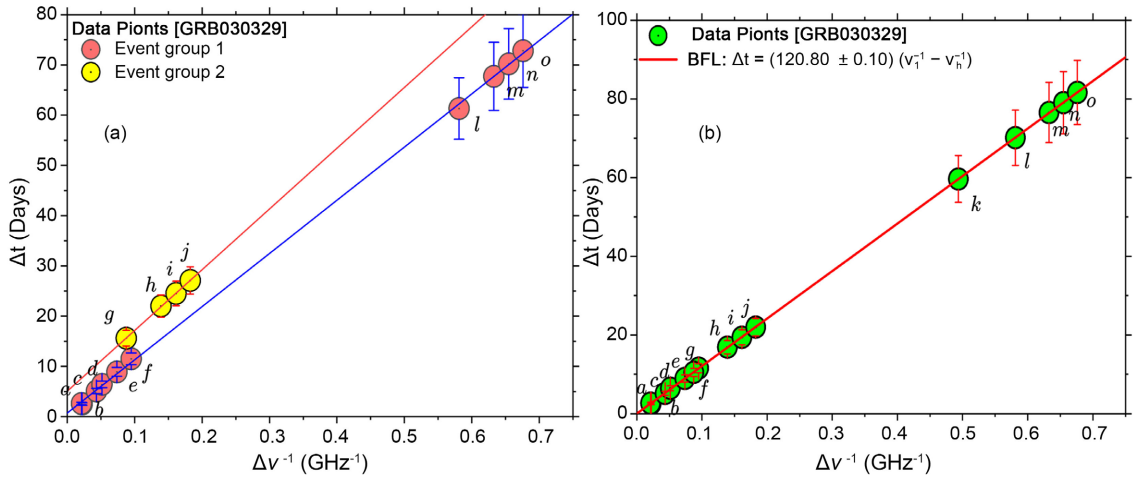

Figure 2. The left panel (a) shows the event grouping 1 and 2 before correction while the right panel (b) shows the combined events after the t_c -correction for **GRB 030329**. Regression fitting for plot (b) gives a correlation coefficient of $r = 1.0000$ indicating a perfect positive correlation between Δt *vs* $\Delta\nu^{-1}$.

b) GRB 980425, as can be seen in the left panel of **Figure 3**, we have (*a*, *c*, *d*) and (*b*, *e*, *f*) forming the two distinct subgroups.

c) GRB 000418, as can be seen in the left panel of **Figure 4**, we have (*a*, *d*) and (*b*, *c*, *e*) forming the two distinct subgroups.

d) GRB 021004, as can be seen in the left panel of **Figure 5**, we have (*a*, *b*, *d*) and (*c*, *e*) forming the two distinct subgroups.

2) Independent regression analysis was carried out on these subgroups. The resulting slopes and intercepts were deduced and are presented in **Table 1**.

3) To "*correct*" for the time delay (t_c), we subtracted the obtained t_c-value from Δt, *i.e.*: $\Delta t \to \Delta t - t_c$. This "*correction*" to the data results in a graph

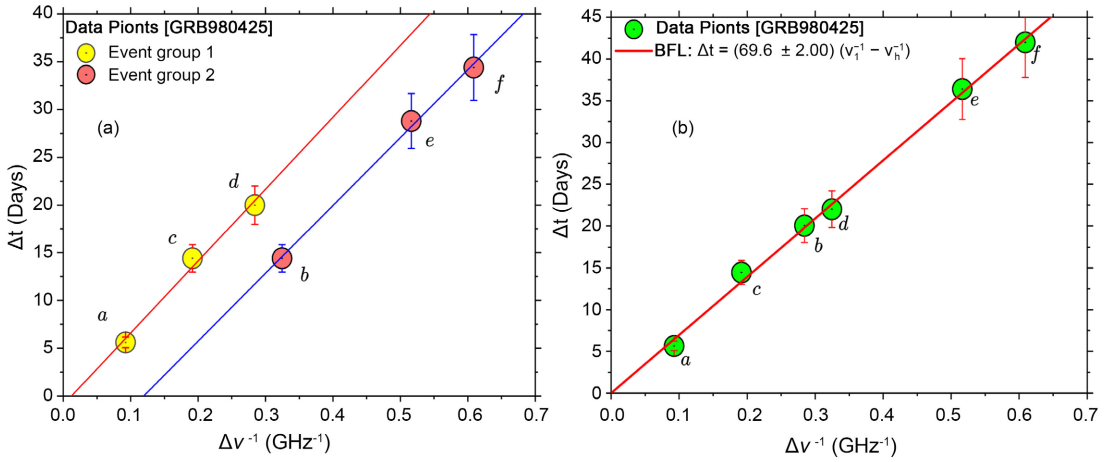

Figure 3. The left panel (a) shows the event grouping 1 and 2 before correction while the right panel (b) shows the combined events after the t_c -correction for **GRB 980425**. Regression fitting for plot (b) gives a correlation coefficient of $r = 0.9986$ indicating a strong positive correlation between Δt *vs* $\Delta \nu^{-1}$.

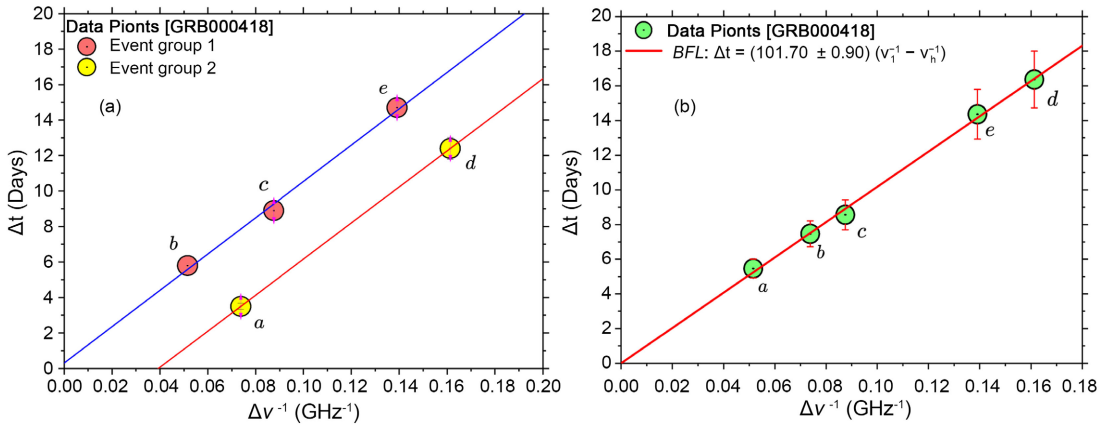

Figure 4. The left panel (a) shows the event grouping 1 and 2 before correction while the right panel (b) shows the combined events after the t_c -correction for **GRB 000418**. Regression fitting for plot (b) gives a correlation coefficient of $r = 0.9998$ indicating a strong positive correlation between Δt *vs* $\Delta \nu^{-1}$.

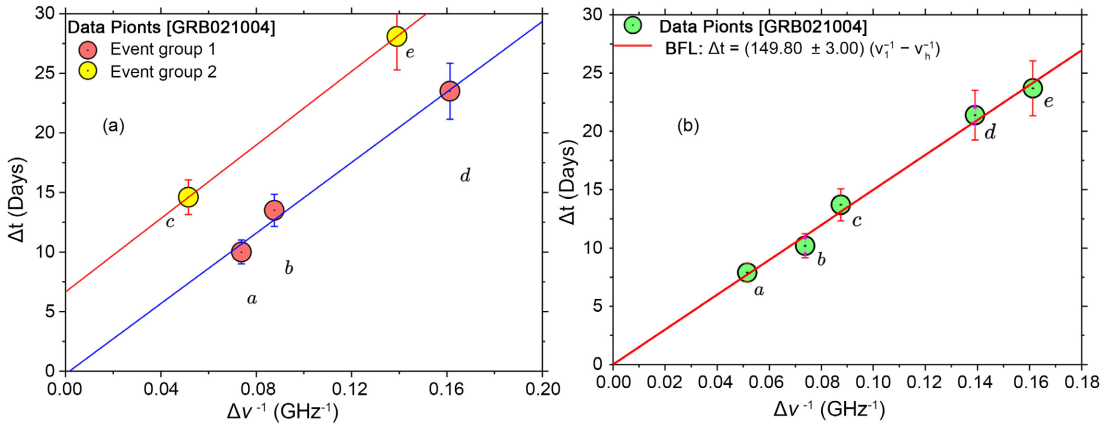

Figure 5. The left panel (a) shows the event grouping 1 and 2 before correction while the right panel (b) shows the combined events after the t_c -correction for **GRB 021004**. Regression fitting for plot (b) gives a correlation coefficient of $r = 0.9994$ indicating a strong positive correlation between Δt *vs* $\Delta \nu^{-1}$.

Table 1. Slopes and time delay corrections for the different GRB subgroups.

Source	Subgroup	Slopes for subgraphs (S_1, S_2) (GHz·Days)	Mean slope (S) (GHz·Days)	y-Intercept (t_c) (t_{c1}, t_{c2}) (Days)
GRB030329	(1)	106.00 ± 0.60	121.00 ± 0.10	+0.70 ± 0.20
	(2)	121.00 ± 2.00		+5.00 ± 0.20
GRB980425	(1)	71.00 ± 4.00	70.00 ± 2.00	−9.00 ± 2.00
	(2)	75.00 ± 8.00		−1.00 ± 2.00
GRB000418	(1)	102.00 ± 0.00	102.00 ± 0.90	−4.00 ± 0.00
	(2)	102.00 ± 7.00		+0.30 ± 0.70
GRB021004	(1)	150.00 ± 20.00	151.00 ± 3.00	−0.30 ± 2.00
	(2)	154.00 ± 0.00		+7.00 ± 0.00

passing through the (0, 0)-point of origin.

4) After instituting the time delay "*correction*" to all four GRBs, we proceeded to plot in Figures 2-5 as a combined graph of the four GRBs showing their event groupings. This was done so that we could see how our regression model fits. Figures 2-5(a) show the combined plot before correction while Figures 2-5(b) show the combined plot after the time delay correction was instituted. Upon a meticulous observation of Figures 2-5(b), one can see that the data points for each of the GRB events have been aligned almost perfectly with the straight line fitting indicating an almost perfect linear correlation.

5.2. Calculation of the Conductance (ν_*) of the ISM

At this point, we must say that, if our model is correct or has any meaningful correspondence with physical and natural reality, then, we are now in a position to obtain ν_*. To that end:

1) First—we note that the slopes of the time delay corrected graphs in the right panels of Figures 2-5, are proportional to the distance to the respective GRBs, *i.e.*:

$$S = \frac{D\nu_*}{c_0}. \tag{24}$$

From this Equation (24), it is clear that if the distance to the GRB is known, the value of ν_* can be computed. Further, if cosmological space is homogeneous, then ν_* must have a constant value in any given cosmological direction that one chooses. Assuming a homogeneous space as is the case in the ΛCDM-model [73], it follows that $S \propto D$, the meaning of which is that if the distance ($D_\dagger$) to just one GRB is known, then, the distance (D_k) to the rest of the GRBs can be inferred from this Equation (24). That is to say: let $S_\dagger$ be the slope on the graph of the GRB whose distance $D_\dagger$ is known and if S_k is the slope on the graph of the GRB whose distance D_k is unknown, then, we can

deduce this distance D_k from the GRB whose slope $S_\dagger$ and distance $D_\dagger$ are known, *i.e.*:

$$D_k = \left(\frac{S_\dagger}{S_k}\right) D_\dagger. \tag{25}$$

From Equation (24), it is abundantly clear that—*in-order to deduce* ν_*—one needs not to know the actual distance to the GRB whose distance $D_\dagger$ is known, but a relative distance—*e.g.*: $D_\dagger \equiv 1$, can be assigned, so that the relative distance $D_{\text{rel}}(k)$, to the k^{th} GRB on our list can be computed, *i.e.*:

$$D_{\text{rel}}(k) = \frac{S_\dagger}{S_k}. \tag{26}$$

From (25) and (26), it follows that:

$$D_k = D_{\text{rel}}(k) D_\dagger. \tag{27}$$

It must be noted that $D_{\text{rel}}(k)$ is a dimensionless quantity while $D_\dagger$ has the dimensions of length.

2) Inserting D_k as given in Equation (27) into Equation (24), where: Δt has been corrected for the non-simultaneous time delay, we will have:

$$\frac{\Delta t}{D_{\text{rel}}} = \frac{D_\dagger \nu_*}{c_0}\left(\frac{1}{\nu_l} - \frac{1}{\nu_h}\right). \tag{28}$$

What Equation (28) implies is that if all our assumptions are correct or have a meaningful correspondence with physical and natural reality, then, a plot of $\Delta t / D_{\text{rel}}$ *vs* $\Delta \nu^{-1}$ should yield a straight line graph.

3) In the present, for our standard GRB with distance $D_\dagger$ and slope $S_\dagger$, we took the GRB with the smallest redshift, namely GRB980425, which has a redshift: $z = 0.009$. The justification for doing this is spelt out in §(7). Therefore, from the foregoing, we have that: $D_\dagger = 40.00 \pm 0.00$ Mpc, and: $S_\dagger = 70.00 \pm 2.00$ GHz · Days. Using the slopes given in **Table 1**, the relative

Table 2. Summary Table: Columns (1)-(8) lists: (1) Source name, (2) Cosmological redshift of the host galaxies [74]-[78], (3) Relative distance (4) Distance to the GRB as obtained from Wright's cosmological calculator (5) Distances to the GRBs as obtained from the present model, (6) Slope of the regression fitting after correction for time delay, (7) The frequency equivalence of the conductance of the ISM as deduced from the graph of each GRB, (8) The coefficient of determination (R^2) which if a function of the strength of the correlation. The last row of the table presents the error-weighted average of the frequency equivalence of the conductance of the ISM.

Source	Host Galaxy Redshift	Relative Distance	$\mathcal{D}_L$ (Mpc)	D_{avg} (Mpc)	$D_\dagger \nu^* / c_0$ (10^{15})	R^2
GRB030329	0.1683 ± 0.0001	1.7360 ± 0.0030	838.9000	69.4000 ± 0.1000	10.0000 ± 0.1000	1.0000
GRB980425	0.0087 ± 0.0000	1.0000 ± 0.0000	40.0000	40.0000 ± 0.0000	6.0000 ± 2.0000	0.9985
GRB000418	1.1181 ± 0.0001	1.4600 ± 0.0100	7804.0000	58.4000 ± 0.4000	9.0000 ± 0.9000	0.9932
GRB021004	2.3304 ± 0.0005	2.1500 ± 0.0300	19188.0000	86.0000 ± 1.0000	13.0000 ± 3.0000	0.9916
			$\nu_* = 1.507 \pm 0.009$			

distances to the GRBs were calculated and are presented in column (3) of Table 2.

4) The value of $\Delta t/D_{\text{rel}}$ for each of the pair of GRB events on our list was computed and plotted against the corresponding $\Delta\nu^{-1}$. To our greatest surprise, all four GRBs yield a straight line and show a very strong and almost perfect correlation. The result of the fitting analysis is shown in Tables A1-4 as well as in the self-explanatory Figure 6. The information presented in the aforementioned tables will be made clear in a subsequent section.

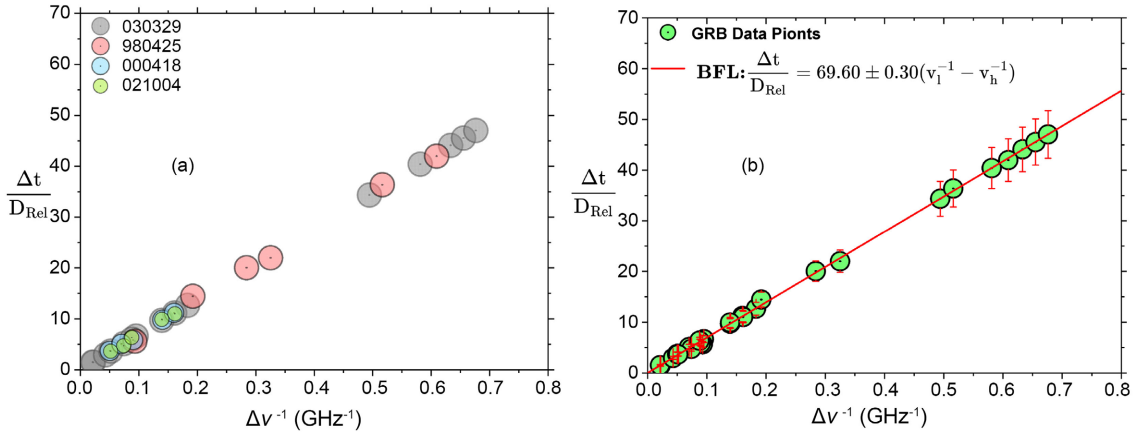

Figure 6. Final plot for GRB 030329, 980425, 000418, 021004 after the relative distance correction: (a) Shows how the four GRBs have aligned perfectly while (b) gives the regression fittings for the combined data points used in obtaining the ν_*. The BFL yield a slope of $(69.60\pm0.30)x-(0.00\pm0.00)$ which implies $t_c=+(0.00\pm0.00)$. The fitting passes through the origin (0, 0) naturally after the corrections were made indicating strong support for our model.

5) On careful observation of Figure 6 one can see that the scatter in the plots has all been fully corrected into an almost perfectly straight line graph. A *t-test* was carried out on the combined plot to test for statistical significance. The result was not only consistent but also significant at a 95% confidence level. The complete regression fittings and other regression parameters are shown in Table 2.

5.3. Data Sampling and Description

As pointed out in Paper 1 [11], our data sample is wholly drawn from [24], wherein [24] draw their data from 304 GRB samples compelled from 1997 to 2011 by [22]. From [24], eight of these GRB samples were used by [11] to investigate correlations in γ-ray burst time delays between pairs of radio photons as paper 1 of a series of research geared towards investigating the cause of time delay in the arrival time of photons of different frequencies emanating from γ-ray burst.

In the said paper 1 [11], in ascending order, the eight distinct GRBs we selected were 980425, 991208 000418, 000926, 021004, 030329, 031203 and 060218 making a total sample size of 52. Amongst these eight GRB samples, four of them GRB 980425, 000418, 021004 and 030329 when applied to our FDSL model

gave good positive linear correlations as expected, which in turn provides a sound basis for our work and reliability of our model. The remaining four samples GRB 991208, 000926, 031203 and 060218 showed a weak correlation, so we didn't include them in our first instalment. In this present instalment, our aim was to put up a working model first with the 4 GRBs that gave a good positive correlation. To avoid constraints, we will differ the remaining weak correlated GRB samples to a later instalment where we can systematically test our model on all the data set in [24]. Additionally, we can now apply this model to recent data.

6. Analysis and Results

Having applied the procedures described in the previous section, we now present an analysis and the results thereof. The strength of the relationship between two or more variables is determined by Pearson's correlation coefficient (r) and the coefficient of determination (R^2) obtained from the scatter plot of the fitting model adopted[2]. From the linear regression fitting procedure, we herein demonstrate a reasonably good linear relation between Δt *vs* $\Delta \nu^{-1}$ for the four GRB Radio-Afterglow emissions. In descending order of the best correlation, as determined by their R^2-value from the linear regression fitting procedure, these are: GRB 030329, GRB 980425, GRB 000418 and GRB 021004. Furthermore, in **Figures 2-5**, plot (*a*) shows the uncorrected event grouping in comparison to plot (*b*) which shows the corrected plots combining the two separate events. For clarity, we have used red circles to represent the uncorrected plot for event group 1, a yellow circle for the uncorrected plot for event group 2 and a green circle for the corrected plot. Additionally, the relative distance plot (1) involving the four GRB combined is represented with green circles which gives the ultimate correction and the value of ν_*.

6.1. GRB 030329

Figure 2 shows a scattered plot of GRB 030329 before and after correction. Regression analysis and fittings in accordance with the FDSL-model yield the following result. Before the correction **Figure 2(a)**, the slope and corresponding R^2 value are 107.00 ± 3.00 and 0.9898 respectively. After correction for time delay **Figure 2(b)**, we have the slope to be 120.80 ± 0.10 and 1.0000. These later results after correction show that the data points have been perfectly aligned thus indicating a good correlation between $\Delta t \propto \Delta \nu^{-1}$.

The significance is that the time delay distances of the GRB data points have been corrected, thus making our fitting model more significant. It is also important to note that such distinct correction greatly improves our result as compared to paper 1. Using the value of ν_* obtained from the *relative distance* correction, we obtain an average distance: $D = 69.40 \pm 0.10$ Mpc when these values are fitted into the FDSL-model. The complete results obtained from our fit-

[2]The R^2 value also captures the Pearson's correlation coefficient for the strength of correlation between the dependent (Δt) and independent variable $\Delta \nu^{-1}$

ting procedures for GRB 030329 are presented in Table A1.

6.2. GRB 980425

In Figure 3, before and after the t_c-correction, we can see that there are six data points for this burst as presented in Table A3. The resulting: Δt *vs* $\Delta\nu^{-1}$, graph for this burst is presented in Figure 3. Before the t_c-correction in Figure 3(a), the results give a reasonable straight line with: $R^2 = 0.932$, and a mean slope: $S = 52.00 \pm 7.00\ \text{GHz}\cdot\text{Days}$. In a more detailed fitting exercise [presented in Figure 3(b)] which was carried out during the correction for time delay, the scatter plot yields a slope of 69.70 ± 2.00 GHz·Days and an R^2 value of 0.997 respectively, indicating a strong correlation. Similarly, the complete results obtained from our fitting procedures for GRB 980425 are presented in Table A3.

6.3. GRB 000418

The graph of: Δt *vs* $\Delta\nu^{-1}$, for this burst is shown in Figure 4. Regression analysis and fitting yield a slope of 100.00 ± 10.00 GHz·Days, and an R^2 value of 0.947 for the uncorrected plot Figure 4(a). On the other hand, the corrected plot in Figure 4(b), yields a slope of 101. ± 1.00 GHz·Days, and an R^2 value of 0.9997, also indicating a strong correlation. Our result for a corrected plot of GRB 000418 fits perfectly as well into our frequency-dependent speed of light model. The average distance to this GRB was estimated to be: $D = 58.40 \pm 0.40\ \text{Mpc}$, when these values are fitted into the FDSL-model. Subsequent information about the event is shown in Table A4.

6.4. GRB 021004

Lastly, the: Δt *vs* $\Delta\nu^{-1}$ graph for GRB 021004 is displayed in Figure 5. Similarly, Table A2 presents the corresponding data for this source for both the corrected and the uncorrected plots. The uncorrected scatter plot in Figure 5(a) gives a slope of 170.00 ± 20.00 GHz·days with an R^2 value of 0.9577. Similarly, the corrected plot in Figure 5(b) gives a slope of 150.00 ± 3.00 GHz·Days and an R^2 value of 0.9988. Using the calculated value for ν_*, we obtain an average distance: $D = 86.00 \pm 1.00\ \text{Mpc}$. Subsequently, values for the conductance and other fitting parameters are presented in Table 2.

6.5. Distances to GRBs

In this section, we compute the luminosity distances to our four GRB samples and their host galaxies using the relation:

$$\mathcal{D}_L = \frac{c_0}{\mathcal{H}_0}\int_0^z \frac{(1+z)\,\mathrm{d}z}{\sqrt{\Omega_\Lambda + \Omega_m (1+z)^3}}, \tag{29}$$

By assuming a flat *Standard* ΛCDM-*Cosmological Model*, we adopt the values for $\Omega_m = 0.315 \pm 0.007$, $\Omega_\Lambda = 0.685 \pm 0.007$ from the Wright's [28] cosmology

[3]http://www.astro.ucla.edu/%7Ewright/CosmoCalc.html: visited on this day: Tuesday 13 March 2024.

online calculator[3], and the present day Hubble parameter [79] as $\mathcal{H}_0 = 67.40 \pm 0.50\ \mathrm{km \cdot s^{-1} \cdot Mpc^{-1}}$. Results of our estimated value for the distances to the four GRBs are displayed in Column 4 of **Table 2**. Alternatively, we also present a model-independent approach to GRB distance estimate using our FSDL model. Our model enables us to infer mathematically the average distances to our GRB samples, wherein we obtain for our four samples an average distance of: ~69.40 ± 0.100, 40.00 ± 0.00, 58.40 ± 0.40, and 86.00 ± 1.00 Mpc, for GRB 030329, 980425, 000418 and 021004, respectively.

7. Summary

A summary table of what has been obtained from the four GRBs is given in **Table 2**. This table not only gives the regression fitting parameters but also demonstrates the potent and latent power of the result obtained if further analysis were to be conducted. The correlation and slopes reveal interesting pointers which may lead to new knowledge in the studies of GRB and estimating distances to them. We shall discuss a few of the possibilities we envisage might be the cause of the time delay and how our newly modified equation fits into the pre-existing model for GRB studies.

For the distances to the GRBs, we can use the ΛCDM-redshift distance estimates. Our reservation with this is that distances deduced using high redshift (*i.e.*, $z > 0.009$) may not be accurate. For example, over the years, there has been a ragging debate on this [80] [81]. This debate has somehow subsided with most astrophysicists and cosmologists accepting the ΛCDM -redshift distance estimates [82]. If any, there have not been any controversy with low redshifts and using these for distance determinations *via* Hubble [59] [83]'s Law.

Rather fortuitously, we have in our four sample GRB the source GRB 980425 with a low redshift of: $z = 0.0090$. This redshift is small enough so much that, one can easily apply the usual *Hubble Law*[4] to determine the distance to this source without the need (*e.g.*) for Wright [28]'s online cosmology calculator. If we can have confidence in the distance to this GRB as determined from Hubble's Law, it means we can safely estimate the the ISM conductance σ. Taking: $\mathcal{H}_0 = 67.4\ \mathrm{km \cdot s^{-1} \cdot Mpc^{-1}}$ [79], we obtain that the source GRB 980425 is at a distance of approximately, $\mathcal{D} = 40\ \mathrm{Mpc}$. Given that for this GRB, we have: $\mathcal{D}\nu_*/c_0 = (6.00 \pm 2.00) \times 10^{15}$, it follows from all this—that, we will have that: $\sigma = (1.0800 \pm 0.0400) \times 10^{-11}\ \Omega^{-1} \cdot \mathrm{m}^{-1}$. If what we have obtained is to be taken seriously, not only are these results consistent, but they also show a great possibility of querying the standard distance method adopted over the years for GRBs using redshift and cosmological methods.

[4]On 26 October 2018, through an electronic vote conducted among all members of the International Astronomical Union (IAU), the resolution to recommend renaming the *Hubble Law* as the *Hubble-Lemaître Law* was accepted. This resolution was proposed in order to pay tribute to both—Georges Henri Joseph Édouard Lemaître (1894-1966), and, Edwin Powell Hubble (1889-1953), for their fundamental contributions to the development of the modern expanding cosmology model.

8. General Discussion and Conclusion

We have herein demonstrated that there exists an impressively strong correlation between the observed time delay and the inverse frequency ($\Delta t \propto \Delta \nu^{-1}$) for a given GRB source and its pair of radio photons. Similarly, for the combined dataset (*i.e.*, GRB 030329, 980425, 000418, 021004) the four GRBs exhibit yet another impressive correlation between $\Delta t / D_{\text{rel}}$ and $\Delta \nu^{-1}$. Of the four GRBs in our case study, not only does GRB 030329 give the best correlation, but this interesting source has the most data points which makes this result statistically significant.

Amongst others, the very fact that we herein obtained an impressive correlation between $\Delta t / D_{\text{rel}}$ and $\Delta \nu^{-1}$ strongly suggests that the present model has an incorrigible element of truth contained in it otherwise, it would be an extremely and very unlikely event and coincidence for this linear correlation to obtain in its present pristine form. If as assumed in the article, the distance to GRB 980425 is to be taken as the standard because we trust the distance estimate to this source as inferred from Hubble's law [59] because its redshift is low enough to be trusted for application using Hubble's law, then, the distance (838.90, 7804.90, 19188.00 Mpc) to the other three sources (*i.e.*, GRB 030329, 000418, 021004) as inferred from the trusted cosmological redshift method is not in agreement with the distance estimates emerging from the present model (69.40, 58.40, 86.00 Mpc).

Of the above-stated discrepancy in the distance measures, we want to categorically state that, we are very much aware that there has in the past been a controversy [see *e.g.* Refs [84]-[91]] regarding the use of redshifts as a distance indicator. For the avoidance of digression and for the sake of focusing our effort on the interesting results emerging from the ongoing study, we decided to defer this issue to a latter instalment where we will dedicate all our effort into putting into perspective our GRB time-delay model as an alternative yardstick for distance measures. This, we strongly felt we needed to make clear to our reader. Lastly, allow us to say that—if this relationship: $\Delta t / D_{\text{rel}}$ *vs* $\Delta \nu^{-1}$, were to be confirmed (or corroborated) for a statistically significant number of GRBs events, it possibly may rule out the Plasma and Photon Mass Effect (which predict: $\Delta t \propto \Delta \nu^{-2}$) as possible candidates for the cause of these GRB time-delays. At any rate, this would be a significant step forward in our understanding of GRBs and the propagation of electromagnetic waves in the cosmos. Our findings and results also underscores the ongoing debate surrounding the internal and external shock mechanisms responsible for GRB emission which we believe is a step forward in the right direction.

Furthermore, as depicted in **Figure 1** we can see that the spatial sizes of the internal and external shocks may also affect the propagation of photons along the jet cone via the ISM. Our findings and results also underscores the ongoing debate surrounding the internal and external shock mechanisms responsible for GRB emission which we believe is a step forward in the right direction. For the

internal shocks, one approach is to consider the variability timescale of the burst, which is related to the spatial size of the emitting region. On the other hand, the external shocks, are formed when the GRB outflow interacts with the surrounding medium, leading to a slower, and more prolonged emission phase. This slowing down of the photons we believe is due to the vast difference between the internal and external shock which our model predicts may be the scatter in our initial plots hence the need for our correction. Additionally, before this time, [92] has already shown that the radius of the external shocks can be estimated based on the deceleration timescale, which depends on the density of the surrounding medium (in this case our hypothesized rarefied plasma medium). His findings agree with our rarefied plasma model as the interactions of the photons and the plasma medium through which these photons travel can significantly affect their propagation, hence leading to the time delay.

9. Conclusions

Now—in conclusion, assuming the correctness of what has been presented herein, we hereby present the following as the yolk of the present findings:

1) The general assumption regarding the emission of GRB photon pairs is that these photons leave the shock front simultaneously. We have shown herein that if this assumption is done away with, one obtains a better correlation in the data variable. As such, we strongly believe that GRB photon pairs do not leave the shock front simultaneously but systematically leave at different times.

2) The combined analysis of the four GRB sources strongly suggests that an independent distance measure to GRBs can be established because the graph of $\Delta t/D_{\text{rel}}$ *vs* $\Delta\nu^{-1}$ supports this position since from this graph we obtain an impressively linear correlation.

3) The strong linear correlation obtained from the graph $\Delta t/D_{\text{rel}}$ *vs* $\Delta\nu^{-1}$, further suggests that the ISM through which these photon pairs move must be homogeneous and this is so because the value of the frequency equivalent of the ISM's conductance is consistent for the four GRBs yielding a mean value of 1.507 ± 0.009 Hz.

4) The fact that the data points of the four GRBs can be grouped into two subgroups suggests that these subgroups may very well be independent shock systems. This needs further investigation and will be subject of our next instalment.

Acknowledgements

We wish to acknowledge the financial support from the Education, Audio and Culture Executive Agency of the European Commission through the Pan-African Planetary and Space Science Network under funding agreement number 6242.24-PANAF-12020-1-BW-PANAF-MOBAF. Also, we would like to acknowledge the invaluable support from our workstations—The Copperbelt University (Republic of Zambia) and the National University of Science and

Technology (Republic of Zimbabwe) for the support rendered in making this work possible.

Data Availability

No new data were generated in support of this research.

Conflicts of Interest

The authors declare no conflicts of interest regarding the publication of this paper.

References

[1] Joshi, J.C., Chand, V. and Razzaque, S. (2023) Synchrotron and Synchrotron Self-Compton Emission Components in GRBs Detected at Very High Energies. *The* 16*th Marcel Grossmann Meeting on Recent Developments in Theoretical and Experimental General Relativity, Astrophysics and Relativistic Field Theories: Proceedings of the MG*16 *Meeting on General Relativity*, 5-10 July 2021, 3009-3016. https://doi.org/10.1142/9789811269776_0243

[2] Huang, Y.F., Lu, T. and Cheng, K.S. (2007) Nonrelativistic Phase in Gamma-Ray Burst After-Glows.

[3] Piro, L., De Pasquale, M., Soffitta, P., Lazzati, D., Amati, L., Costa, E., *et al.* (2005) Probing the Environment in Gamma-Ray Bursts: The Case of an X-Ray Precursor, Afterglow Late Onset, and Wind versus Constant Density Profile in GRB 011121 and GRB 011211. *The Astrophysical Journal*, **623**, 314-324. https://doi.org/10.1086/428377

[4] Zou, Z.C., Zhang, B.B., Huang, Y.F. and Zhao, X.H. (2021) Gamma-Ray Burst in a Binary System. *The Astrophysical Journal*, **921**, 2. https://doi.org/10.3847/1538-4357/ac1b2d

[5] Janiuk, A., James, B. and Sapountzis, K. (2021) Cosmic Gamma Ray Bursts. *Acta Physica Polonica A*, **139**, 273-276. https://doi.org/10.12693/aphyspola.139.273

[6] Bromberg, O., Nakar, E. and Piran, T. (2011) Are Low-Luminosity Gamma-Ray Bursts Generated by Relativistic Jets? *The Astrophysical Journal*, **739**, L55. https://doi.org/10.1088/2041-8205/739/2/l55

[7] Konigl, A. (1981) Relativistic Jets as X-Ray and Gamma-Ray Sources. *The Astrophysical Journal*, **243**, 700-709. https://doi.org/10.1086/158638

[8] Kumar, P. and Zhang, B. (2015) The Physics of Gamma-Ray Bursts & Relativistic Jets. *Physics Reports*, **561**, 1-109. https://doi.org/10.1016/j.physrep.2014.09.008

[9] Ciolfi, R. (2018) Short Gamma-Ray Burst Central Engines. *International Journal of Modern Physics D*, **27**, Article ID: 1842004. https://doi.org/10.1142/s021827181842004x

[10] Levan, A.J., Tanvir, N.R., Starling, R.L.C., Wiersema, K., Page, K.L., Perley, D.A., *et al.* (2013) A New Population of Ultra-Long Duration Gamma-Ray Bursts. *The Astrophysical Journal*, **781**, Article No. 13. https://doi.org/10.1088/0004-637x/781/1/13

[11] Nyambuya, G.G., Marusenga, S., Abbey, G.F., Simpemba, P. and Simfukwe, J. (2023) Correlation in Gamma Ray Burst Time Delays between Pairs of Radio Photons. *International Journal of Astronomy and Astrophysics*, **13**, 195-216.

[12] Hao, J. and Yuan, Y. (2013) Progenitor Delay-Time Distribution of Short Gamma-Ray Bursts: Constraints from Observations. *Astronomy & Astrophysics*, **558**,

A22. https://doi.org/10.1051/0004-6361/201321471

[13] Zhang, B. and Zhang, B. (2014) Gamma-Ray Burst Prompt Emission Light Curves and Power Density Spectra in the ICMART Model. *The Astrophysical Journal*, **782**, Article No. 92. https://doi.org/10.1088/0004-637x/782/2/92

[14] Albert, J., Aliu, E., Anderhub, H., Antonelli, L.A., Antoranz, P., Backes, M., *et al.* (2008) Probing Quantum Gravity Using Photons from a Flare of the Active Galactic Nucleus Markarian 501 Observed by the MAGIC Telescope. *Physics Letters B*, **668**, 253-257. https://doi.org/10.1016/j.physletb.2008.08.053

[15] Martínez, M. and Errando, M. (2009) A New Approach to Study Energy-Dependent Arrival Delays on Photons from Astrophysical Sources. *Astroparticle Physics*, **31**, 226-232. https://doi.org/10.1016/j.astropartphys.2009.01.005

[16] Zhang, B. (2019) The Delay Time of Gravitational Wave—Gamma-Ray Burst Associations. *Frontiers of Physics*, **14**, Article No. 64402. https://doi.org/10.1007/s11467-019-0913-4

[17] Farias, K.E.L.d., Sampaio, T.A.M., Anacleto, M.A., Brito, F.A. and Passos, E. (2021) Lifshitz Scaling in CPT-Even Lorentz-Violating Electrodynamics and GRB Time Delay. *The European Physical Journal Plus*, **136**, Article No. 257. https://doi.org/10.1140/epjp/s13360-021-01228-y

[18] Wijers, R.A.M.J., Bloom, J.S., Bagla, J.S. and Natarajan, P. (1998) Gamma-Ray Bursts from Stellar Remnants: Probing the Universe at High Redshift. *Monthly Notices of the Royal Astronomical Society*, **294**, L13-L17. https://doi.org/10.1046/j.1365-8711.1998.01328.x

[19] Salam, A. and Ward, J.C. (1959) Weak and Electromagnetic Interactions. *Il Nuovo Cimento*, **11**, 568-577. https://doi.org/10.1007/bf02726525

[20] Salmon, L., Hanlon, L. and Martin-Carrillo, A. (2022) Two Classes of Gamma-Ray Bursts Distinguished within the First Second of Their Prompt Emission. *Galaxies*, **10**, Article No. 78. https://doi.org/10.3390/galaxies10040078

[21] Lazzati, D. (2020) Short Duration Gamma-Ray Bursts and Their Outflows in Light of Gw170817. *Frontiers in Astronomy and Space Sciences*, **7**, Article ID: 578849. https://doi.org/10.3389/fspas.2020.578849

[22] Chandra, P. and Frail, D.A. (2012) A Radio-Selected Sample of Gamma-Ray Burst Afterglows. *The Astrophysical Journal*, **746**, Article No. 156. https://doi.org/10.1088/0004-637x/746/2/156

[23] Matheson, T., Garnavich, P.M., Foltz, C., West, S., Williams, G., Falco, E., *et al.* (2002) The Spectroscopic Variability of GRB 021004. *The Astrophysical Journal*, **582**, L5-L9. https://doi.org/10.1086/367601

[24] Zhang, B., Chai, Y., Zou, Y. and Wu, X. (2016) Constraining the Mass of the Photon with Gamma-Ray Bursts. *Journal of High Energy Astrophysics*, **11**, 20-28. https://doi.org/10.1016/j.jheap.2016.07.001

[25] Aleksic, J., Alvarez, E.A., Antonelli, L.A., Antoranz, P., Asensio, M., Backes, M., *et al.* (2012) PG 1553+113: Five Years of Observations with MAGIC. *The Astrophysical Journal*, **748**, Article No. 46.

[26] Proca, A. (1936) Sur la Théorie du Positron. *Comptes Rendus de l'Académie des Sciences*, **202**, 1366-1368.

[27] Abdo, A., Ackermann, M., Ajello, M., Allafort, A., Baldini, L., Ballet, J., *et al.* (2011) Insights into the High-Energy γ-Ray Emission of Markarian 501 from Extensive Multifrequency Observations in the Fermi Era. *ApJ*, **727**, Article No. 129.

[28] Wright, E.L. (2006) A Cosmology Calculator for the World Wide Web. *Publications*

of the Astronomical Society of the Pacific, **118**, 1711-1715. https://doi.org/10.1086/510102

[29] Planck Collaboration, Ade, P.A.R., Aghanim, N., Alves, M.I.R., Armitage-Caplan, C., Arnaud, M., *et al.* (2014) Planck 2013 Results. I. Overview of Products and Scientific Results. *A&A*, **571**, A1.

[30] Wijers, R.A.M.J. and Paczynski, B. (1994) On the Nature of Gamma-Ray Burst Time Dilations. *The Astrophysical Journal*, **437**, L107. https://doi.org/10.1086/187694

[31] Paczynski, B. (1986) Gamma-Ray Bursters at Cosmological Distances. *The Astrophysical Journal*, **308**, L43-L46. https://doi.org/10.1086/184740

[32] Lamb, D.Q. (1995) The Distance Scale to Gamma-Ray Bursts. *Publications of the Astronomical Society of the Pacific*, **107**, 1152. https://doi.org/10.1086/133673

[33] Narayan, R., Paczynski, B. and Piran, T. (1992) Gamma-Ray Bursts as the Death Throes of Massive Binary Stars. *The Astrophysical Journal*, **395**, L83-L86. https://doi.org/10.1086/186493

[34] Fishman, G.J. and Meegan, C.A. (1995) Gamma-Ray Bursts. *Annual Review of Astronomy and Astrophysics*, **33**, 415-458. https://doi.org/10.1146/annurev.aa.33.090195.002215

[35] Khadka, N., Luongo, O., Muccino, M. and Ratra, B. (2021) Do Gamma-Ray Burst Measurements Provide a Useful Test of Cosmological Models? *Journal of Cosmology and Astroparticle Physics*, **9**, 42. https://doi.org/10.1088/1475-7516/2021/09/042

[36] Laviolette, P.A. (1986) Is the Universe Really Expanding? *The Astrophysical Journal*, **301**, 544-553. https://doi.org/10.1086/163922

[37] Amati, L., Frontera, F., Tavani, M., Antonelli, A., Costa, E., *et al.* (2002) Intrinsic Spectra and Energetics of Bepposax Gamma-Ray Bursts with Known Redshifts. *Astronomy & Astrophysics*, **390**, 81-89. https://doi.org/10.1051/0004-6361:20020722

[38] Horváth, I., Hakkila, J. and Bagoly, Z. (2014) Possible Structure in the GRB Sky Distribution at Redshift Two. *Astronomy & Astrophysics*, **561**, L12. https://doi.org/10.1051/0004-6361/201323020

[39] Ukwatta, T.N. and Woźniak, P.R. (2015) Investigation of Redshift- and Duration-Dependent Clustering of Gamma-Ray Bursts. *Monthly Notices of the Royal Astronomical Society*, **455**, 703-711. https://doi.org/10.1093/mnras/stv2350

[40] Xiao, L. and Schaefer, B.E. (2009) Estimating Redshifts for Long Gamma-Ray Bursts. *The Astrophysical Journal*, **707**, 387-403. https://doi.org/10.1088/0004-637x/707/1/387

[41] Yonetoku, D., Murakami, T., Nakamura, T., Yamazaki, R., Inoue, A.K. and Ioka, K. (2004) Gamma-Ray Burst Formation Rate Inferred from the Spectral Peak Energy-Peak Luminosity Relation. *The Astrophysical Journal*, **609**, 935-951. https://doi.org/10.1086/421285

[42] Holanda, R.F.L., Busti, V.C., Lima, F.S. and Alcaniz, J.S. (2017) Probing the Distance-Duality Relation with High-Z Data. *Journal of Cosmology and Astroparticle Physics*, **9**, 39. https://doi.org/10.1088/1475-7516/2017/09/039

[43] Yang, T., Holanda, R.F.L. and Hu, B. (2019) Constraints on the Cosmic Distance Duality Relation with Simulated Data of Gravitational Waves from the Einstein Telescope. *Astroparticle Physics*, **108**, 57-62. https://doi.org/10.1016/j.astropartphys.2019.01.005

[44] Řípa, J., Mészáros, A. and Ryde, F. (2011) Cosmological Effects on the Observed Flux and Fluence Distributions of Gamma-Ray Bursts. *Proceedings of the Interna-*

tional Astronomical Union, **7**, 385-386. https://doi.org/10.1017/s1743921312013464

[45] Zaninetti, L. (2016) The Truncated Lognormal Distribution as a Luminosity Function for SWIFT-BAT Gamma-Ray Bursts. *Galaxies*, **4**, Article No. 57. https://doi.org/10.3390/galaxies4040057

[46] Bonetti, L., Ellis, J., Mavromatos, N.E., Sakharov, A.S., Sarkisyan-Grinbaum, E.K. and Spallicci, A.D.A.M. (2017) FRB 121102 Casts New Light on the Photon Mass. *Physics Letters B*, **768**, 326-329. https://doi.org/10.1016/j.physletb.2017.03.014

[47] Bonetti, L., Ellis, J., Mavromatos, N.E., Sakharov, A.S., Sarkisyan-Grinbaum, E.K. and Spallicci, A.D.A.M. (2016) Photon Mass Limits from Fast Radio Bursts. *Physics Letters B*, **757**, 548-552. https://doi.org/10.1016/j.physletb.2016.04.035

[48] Shao, L. and Zhang, B. (2017) Bayesian Framework to Constrain the Photon Mass with a Catalog of Fast Radio Bursts. *Physical Review D*, **95**, Article ID: 123010. https://doi.org/10.1103/physrevd.95.123010

[49] Wu, X., Zhang, S., Gao, H., Wei, J., Zou, Y., Lei, W., *et al.* (2016) Constraints on the Photon Mass with Fast Radio Bursts. *The Astrophysical Journal Letters*, **822**, L15. https://doi.org/10.3847/2041-8205/822/1/l15

[50] Einstein, A. (1917) Kosmologische Betrachtungen zur allgemeinen Relativitatstheorie. Preussische Akademie der Wissenschaften, Sitzungsberichte (Part 1). Document ID: MPIWG: H428RSAN. Einstein's Seminal Paper on Cosmology Heralding the Genesis of the Scientific Exploration of Physical Cosmology, 142-152.

[51] Einstein, A. (1915) Grundgedanken der allgemeinen Relativitatstheorie und Anwendung dieser Theorie in der Astronomie (Fundamental Ideas of the General Theory of Relativity and the Application of This Theory in Astronomy). Preussische Akademie der Wissenschaften, Sitzungsberichte (Part 1), 315.

[52] Einstein, A. (1915) Zur allgemeinen Relativitatstheorie (On the General Theory of Relativity). Preussische Akademie der Wissenschaften, Sitzungsberichte (Part 2), 778-786, 799-801.

[53] Friedmann, A. (1924) Über die Möglichkeit einer Welt mit konstanter negativer Krümmung des Raumes. *Zeitschrift für Physik*, **21**, 326-332. https://doi.org/10.1007/bf01328280

[54] Lemaıtre, G. (1933) Über die Krümmung des Raumes. *Annales de la Socie'te' Scientifique de Bruxelles*, **A53**, 51-85.

[55] Robertson, H.P. (1936) Kinematics and World-Structure II. *The Astrophysical Journal*, **83**, 187-201. https://doi.org/10.1086/143716

[56] Robertson, H.P. (1936) Kinematics and World-Structure III. *The Astrophysical Journal*, **83**, 257-271. https://doi.org/10.1086/143726

[57] Robertson, H.P. (1935) Kinematics and World-Structure. *The Astrophysical Journal*, **82**, 284-301. https://doi.org/10.1086/143681

[58] Walker, A.G. (1937) On Milne's Theory of World-Structure. *Proceedings of the London Mathematical Society*, **s2-42**, 90-127. https://doi.org/10.1112/plms/s2-42.1.90

[59] Hubble, E. (1929) A Relation between Distance and Radial Velocity among Extra-Galactic Nebulae. *Proceedings of the National Academy of Sciences*, **15**, 168-173. https://doi.org/10.1073/pnas.15.3.168

[60] Lemaıtre, G. (1927) Un univers Homog'ene de Masse Constante et de Rayon Croissant Rendant Compte de la Vitesse Radiale des N'ebuleuses Extragalactiques (A Homogeneous Universe of Constant Mass and Increasing Radius Accounting for the Radial Velocity of Extragalactic Nebulae). *Annales de la Soci'et'e Scientifique de*

Bruxelles, **A47**, 49-59.

[61] Taylor, G.B., Frail, D.A., Berger, E. and Kulkarni, S.R. (2004) The Angular Size and Proper Motion of the Afterglow of GRB 030329. *The Astrophysical Journal*, **609**, L1-L4. https://doi.org/10.1086/422554

[62] Eichler, D. and Levinson, A. (2000) A Compact Fireball Model of Gamma-Ray Bursts. *The Astrophysical Journal*, **529**, 146-150. https://doi.org/10.1086/308245

[63] Piran, T. (1999) Gamma-Ray Bursts and the Fireball Model. *Physics Reports*, **314**, 575-667. https://doi.org/10.1016/s0370-1573(98)00127-6

[64] Fox, D.B. and Mészáros, P. (2006) GRB Fireball Physics: Prompt and Early Emission. *New Journal of Physics*, **8**, 199-199. https://doi.org/10.1088/1367-2630/8/9/199

[65] Thompson, C. (1994) A Model of Gamma-Ray Bursts. *Monthly Notices of the Royal Astronomical Society*, **270**, 480-498. https://doi.org/10.1093/mnras/270.3.480

[66] Pe'er, A. (2015) Physics of Gamma-Ray Bursts Prompt Emission. *Advances in Astronomy*, **2015**, Article ID: 907321. https://doi.org/10.1155/2015/907321

[67] Piran, T. (2005) The Physics of Gamma-Ray Bursts. *Reviews of Modern Physics*, **76**, 1143-1210. https://doi.org/10.1103/revmodphys.76.1143

[68] Yost, S.A., Harrison, F.A., Sari, R. and Frail, D.A. (2003) A Study of the Afterglows of Four Gamma-Ray Bursts: Constraining the Explosion and Fireball Model. *The Astrophysical Journal*, **597**, 459-473. https://doi.org/10.1086/378288

[69] Mészáros, P. (2000) The Fireball Shock Model of Gamma Ray Bursts. *AIP Conference Proceedings*, **522**, 213-225. https://doi.org/10.1063/1.1291716

[70] Oates, S.R., Page, M.J., Schady, P., de Pasquale, M., Koch, T.S., Breeveld, A.A., *et al.* (2009) A Statistical Study of Gamma-Ray Burst Afterglows Measured by the Swift Ultraviolet Optical Telescope. *Monthly Notices of the Royal Astronomical Society*, **395**, 490-503. https://doi.org/10.1111/j.1365-2966.2009.14544.x

[71] Yu, Y.-W., Gao, H., Wang, F.-Y. and Zhang, B.-B. (2022) Gamma-Ray Bursts.

[72] Dado, S., Dar, A. and De Rújula, A. (2022) Critical Tests of Leading Gamma Ray Burst Theories. *Universe*, **8**, Article No. 350. https://doi.org/10.3390/universe8070350

[73] Fay, S. (2020) ΛCDM Periodic Cosmology. *Monthly Notices of the Royal Astronomical Society*, **494**, 2183-2190. https://doi.org/10.1093/mnras/staa940

[74] Stanek, K.Z., Matheson, T., Garnavich, P.M., Martini, P., Berlind, P., Caldwell, N., *et al.* (2003) Spectroscopic Discovery of the Supernova 2003dh Associated with GRB 030329. *The Astrophysical Journal*, **591**, L17-L20. https://doi.org/10.1086/376976

[75] Hurley, K., Sommer, M., Atteia, J.-L., Boer, M., Cline, T., Cotin, F., *et al.* (1992) The Solar X-Ray/Cosmic Gamma-Ray Burst Experiment Aboard Ulysses. *Astronomy and Astrophysics Supplement Series*, **92**, 401-410.

[76] Bloom, J.S., Berger, E., Kulkarni, S.R., Djorgovski, S.G. and Frail, D.A. (2003) The Redshift Determination of GRB 990506 and GRB 000418 with the Echellete Spectrograph Imager on Keck. *The Astronomical Journal*, **125**, 999-1005. https://doi.org/10.1086/367805

[77] Klose, S., Stecklum, B., Masetti, N., Pian, E., Palazzi, E., Henden, A.A., *et al.* (2000) The Very Red Afterglow of GRB 000418: Further Evidence for Dust Extinction in a Gamma-Ray Burst Host Galaxy. *The Astrophysical Journal*, **545**, 271-276. https://doi.org/10.1086/317816

[78] Waxman, E. (2004) The Nature of GRB 980425 and the Search for Off-Axis Gamma-Ray Burst Signatures in Nearby Type Ib/c Supernova Emission. *The Astrophys-*

ical Journal, **602**, 886-891. https://doi.org/10.1086/381230

[79] Alves, J., Forveille, T., Pentericci, L. and Shore, S. (2020) Planck 2018 Results-VI. Cosmological Parameters. *Astronomy & Astrophysics*, **641**, A6. https://doi.org/10.1051/0004-6361/202039265

[80] Parker, B. (1993) The Redshift Controversy. In: *The Vindication of the Big Bang: Breakthroughs and Barriers*, Springer, 281-300.

[81] Lian, Y., Cao, S., Biesiada, M., Chen, Y., Zhang, Y. and Guo, W. (2021) Probing Modified Gravity Theories with Multiple Measurements of High-Redshift Quasars. *Monthly Notices of the Royal Astronomical Society*, **505**, 2111-2123. https://doi.org/10.1093/mnras/stab1373

[82] Salpeter, E.E. and Hoffman, G.L. (1986) The Galaxy Luminosity Function and the Redshift-Distance Controversy (A Review). *Proceedings of the National Academy of Sciences*, **83**, 3056-3063. https://doi.org/10.1073/pnas.83.10.3056

[83] Davis, T. (2019) An Expanding Controversy. *Science*, **365**, 1076-1077. https://doi.org/10.1126/science.aay1331

[84] Arp, H. (1967) Peculiar Galaxies and Radio Sources. *The Astrophysical Journal*, **148**, 321-366. https://doi.org/10.1086/149159

[85] Arp, H. (1966) Atlas of Peculiar Galaxies. *The Astrophysical Journal Supplement Series*, **14**, 1-20. https://doi.org/10.1086/190147

[86] Arp, H. (1981) Quasars near Companion Galaxies. *The Astrophysical Journal*, **250**, 31-42. https://doi.org/10.1086/159345

[87] Arp, H.C. (1988) Quasars, Redshifts and Controversies. Cambridge University Press.

[88] Karlsson, K.G. (1977) On the Existence of Significant Peaks in the Quasar Redshift Distribution. *Astronomy and Astrophysics*, **58**, 237-240.

[89] Tang, S.M. and Zhang, S.N. (2005) Critical Examinations of QSO Redshift Periodicities and Associations with Galaxies in Sloan Digital Sky Survey Data. *The Astrophysical Journal*, **633**, 41-51. https://doi.org/10.1086/432754

[90] Bell, M.B. and McDiarmid, D. (2006) Six Peaks Visible in the Redshift Distribution of 46,400 SDSS Quasars Agree with the Preferred Redshifts Predicted by the Decreasing Intrinsic Redshift Model. *The Astrophysical Journal*, **648**, 140-147. https://doi.org/10.1086/503792

[91] Ratcliffe, H. (2010) Anomalous Redshift Data and the Myth of Cosmological Distance. *Journal of Cosmology*, **4**, 693-718.

[92] Sari, R. and Piran, T. (1995) Hydrodynamic Timescales and Temporal Structure of Gamma-Ray Bursts. *The Astrophysical Journal*, **455**, L143-L146. https://doi.org/10.1086/309835

Appendix

Table A1. Data Table for GRB 030329. From this data—according to our fitting analysis in **Figure 2**, we obtain: $\frac{D\nu_*}{c_0} = (10.40 \pm 0.10) \times 10^{15}$.

GRB Event Label	ν_1 (GHz)	ν_2 (GHz)	t_1 4 (Days)	t_2 (Days)	$\Delta\nu^{-1}$ (GHz^{-1})	Δt (Days)	Δt_c (Days)	$\Delta t_c / D_{\text{rel}}$ (Days)
a	15.00	22.50	8.40	10.90	0.022	2.50	3.00 ± 0.30	2.00 ± 0.10
b	22.50	43.00	5.80	8.40	0.021	2.60	3.00 ± 0.30	2.00 ± 0.20
c	15.00	43.00	5.80	10.90	0.043	5.10	5.00 ± 0.50	3.00 ± 0.30
d	8.46	15.00	10.90	17.30	0.052	6.40	6.00 ± 0.60	4.00 ± 0.40
e	8.46	22.50	8.40	17.30	0.074	8.90	9.00 ± 1.00	5.00 ± 0.50
f	8.46	43.00	5.80	17.30	0.095	11.50	12.00 ± 1.00	7.00 ± 0.70
g	4.86	8.46	17.30	32.90	0.088	15.60	11.00 ± 2.00	6.00 ± 0.60
h	4.86	15.00	10.90	32.90	0.139	22.00	17.00 ± 2.00	10.00 ± 1.00
i	4.86	22.50	8.40	32.90	0.161	24.50	19.00 ± 3.00	11.00 ± 1.00
j	4.86	43.00	5.80	32.90	0.183	27.10	22.00 ± 3.00	13.00 ± 1.00
k	1.43	4.86	32.90	78.60	0.494	45.70	60.00 ± 5.00	34.00 ± 3.00
l	1.43	8.46	17.30	78.60	0.581	61.30	70.00 ± 6.00	40.00 ± 4.00
m	1.43	15.00	10.90	78.60	0.633	67.70	77.00 ± 7.00	44.00 ± 4.00
n	1.43	22.50	8.40	78.60	0.655	70.20	79.00 ± 7.00	46.00 ± 5.00
o	1.43	43.00	5.80	78.60	0.676	72.80	82.00 ± 7.00	47.00 ± 5.00

Table A2. Data Table for GRB021004. From this data—according to **Figure 5**, we obtain: $\frac{D\nu_*}{c_0} = (12.90 \pm 3.00) \times 10^{15}$.

GRB Event Label	ν_1 (GHz)	ν_2 (GHz)	t_1 (Days)	t_2 (Days)	$\Delta\nu^{-1}$ (GHz^{-1})	Δt (Days)	Δt_c (Days)	$\Delta t_c / D_{\text{rel}}$ (Days)
a	22.50	8.46	8.70	18.70	0.07	10.00	10.00 ± 1.00	5.00 ± 0.50
b	8.46	4.86	18.70	32.20	0.09	13.50	14.00 ± 1.00	6.00 ± 0.60
d	22.50	4.86	8.70	32.20	0.16	23.50	24.00 ± 2.00	11.00 ± 1.00
c	15.00	8.46	4.10	18.70	0.05	14.600	9.00 ± 0.80	4.00 ± 0.40
e	15.00	4.86	4.10	32.20	0.14	28.10	21.00 ± 2.00	10.00 ± 1.00

Table A3. Data Table for GRB 980425. From this data—according to our fitting analysis in **Figure 3**, we obtain: $\frac{D\nu_*}{c_0} = (6.00 \pm 2.00) \times 10^{15}$.

GRB Event Label	ν_1 (GHz)	ν_2 (GHz)	t_1 (Days)	t_2 (Days)	$\Delta\nu^{-1}$ (GHz^{-1})	Δt (Days)	Δt_c (Days)	$\Delta t_c / D_{\text{rel}}$ (Days)
a	4.80	8.64	12.70	18.30	0.09	5.64	6.00 ± 0.60	6.00 ± 0.60
c	2.50	4.80	18.30	32.70	0.19	14.44	14.00 ± 1.00	14.00 ± 1.00
d	2.50	8.64	12.70	32.70	0.28	20.04	20.00 ± 2.00	20.00 ± 2.00
b	1.38	2.50	32.70	47.10	0.33	14.44	22.00 ± 2.00	22.00 ± 2.00
e	1.38	4.80	18.30	47.10	0.52	28.84	36.00 ± 4.00	36.00 ± 4.00
f	1.38	8.64	12.70	47.10	0.61	34.44	42.00 ± 4.00	42.00 ± 4.00

Table A4. Data Table for GRB 000418. From this data—according to our fitting analysis in **Figure 4**, we obtain: $\frac{Dv_*}{c_0} = (8.804 \pm 0.90) \times 10^{15}$.

GRB Event Label	v_1 (GHz)	v_2 (GHz)	t_1 (Days)	t_2 (Days)	Δv^{-1} (GHz^{-1})	Δt (Days)	Δt_c (Days)	$\Delta t_c / D_{\text{rel}}$ (Days)
e	4.86	15.00	12.30	27.00	0.14	14.700	14.00 ± 1.00	10.00 ± 1.00
b	8.46	15.00	12.30	18.10	0.05	5.800	6.00 ± 0.50	4.00 ± 0.40
c	4.86	8.46	18.10	27.00	0.09	8.900	9.00 ± 0.90	6.00 ± 0.60
d	4.86	22.50	14.60	27.00	0.16	12.400	16.00 ± 2.00	11.00 ± 1.00
a	8.46	22.50	14.60	18.10	0.07	3.500	8.00 ± 0.70	5.00 ± 0.50

Table A5. Combined Data Table [25]: Columns (1)-(8) list the (1) Initial/low frequency of the burst, (2) Final/high frequency of the burst (3) Initial time of the burst (4) Final time of the burst (5) Difference in the frequency (6) Values obtain from the two-fold correction (7) Relative distance obtained from the slopes of the four GRBs (8) Final values obtained from the relative distance correction.

GRB Event Label	v_1 (GHz)	v_2 (GHz)	t_1 (Days)	t_2 (Days)	Δv^{-1} (GHz^{-1})	Δt_c (Days)	D_{rel}	$\Delta t_c / D_{\text{rel}}$ (Days)
GRB030329a	15.00	22.50	8.40	10.90	0.022	2.56	1.7360 ± 0.0030	2.00 ± 0.10
GRB030329b	22.50	43.00	5.80	8.40	0.021	2.64	1.7360 ± 0.0030	2.00 ± 0.20
GRB030329c	15.00	43.00	5.80	10.90	0.043	5.14	1.7360 ± 0.0030	3.00 ± 0.30
GRB030329d	8.46	15.00	10.90	17.30	0.052	6.44	1.7360 ± 0.0030	4.00 ± 0.40
GRB030329e	8.46	22.50	8.40	17.30	0.074	8.94	1.7360 ± 0.0030	5.00 ± 0.50
GRB030329f	8.46	43.00	5.80	17.30	0.095	11.54	1.7360 ± 0.0030	7.00 ± 0.70
GRB030329g	4.86	8.46	17.30	32.90	0.088	10.49	1.7360 ± 0.0030	6.00 ± 0.60
GRB030329h	4.86	15.00	10.90	32.90	0.139	16.89	1.7360 ± 0.0030	10.00 ± 1.00
GRB030329i	4.86	22.50	8.40	32.90	0.161	19.39	1.7360 ± 0.0030	11.00 ± 1.00
GRB030329j	4.86	43.00	5.80	32.90	0.183	21.99	1.7360 ± 0.0030	13.00 ± 1.00
GRB030329k	1.43	4.86	32.90	78.60	0.494	59.65	1.7360 ± 0.0030	34.00 ± 3.00
GRB030329l	1.43	8.46	17.30	78.60	0.581	70.15	1.7360 ± 0.0030	40.00 ± 4.00
GRB030329m	1.43	15.00	10.90	78.60	0.633	76.55	1.7360 ± 0.0030	44.00 ± 4.00
GRB030329n	1.43	22.50	8.40	78.60	0.655	79.05	1.7360 ± 0.0030	46.00 ± 5.00
GRB030329o	1.43	43.00	5.80	78.60	0.676	81.65	1.7360 ± 0.0030	47.00 ± 5.00
GRB980425a	4.80	8.64	12.70	18.30	0.093	5.65	1.0000 ± 0.0000	6.00 ± 0.60
GRB980425c	2.50	4.80	18.30	32.70	0.192	14.45	1.0000 ± 0.0000	14.00 ± 1.00
GRB980425d	2.50	8.64	12.70	32.70	0.284	20.05	1.0000 ± 0.0000	20.00 ± 2.00
GRB980425b	1.38	2.50	32.70	47.10	0.325	21.60	1.0000 ± 0.0000	22.00 ± 2.00
GRB980425e	1.38	4.80	18.30	47.10	0.516	36.40	1.0000 ± 0.0000	36.00 ± 4.00
GRB980425f	1.38	8.64	12.70	47.10	0.609	42.00	1.0000 ± 0.0000	42.00 ± 4.00
GRB000418e	4.86	15.00	12.30	27.00	0.140	14.36	1.4600 ± 0.0100	10.00 ± 1.00
GRB000418b	8.46	15.00	12.30	18.10	0.050	5.46	1.4600 ± 0.0100	4.00 ± 0.40
GRB000418c	4.86	8.46	18.10	27.00	0.090	8.56	1.4600 ± 0.0100	6.00 ± 0.60
GRB000418d	4.86	22.50	14.60	27.00	0.160	16.37	1.4600 ± 0.0100	11.00 ± 1.00
GRB000418a	8.46	22.50	14.60	18.10	0.070	7.47	1.4600 ± 0.0100	5.00 ± 0.50
GRB021004a	8.46	22.50	8.70	18.70	0.074	10.2	2.1500 ± 0.0300	5.00 ± 0.50
GRB021004b	4.86	8.46	18.70	32.20	0.088	13.7	2.1500 ± 0.0300	6.00 ± 0.60
GRB021004d	4.86	22.50	8.70	32.20	0.161	23.7	2.1500 ± 0.0300	11.00 ± 1.00
GRB021004c	8.46	15.00	4.10	18.70	0.052	7.89	2.1500 ± 0.0300	4.00 ± 0.40
GRB021004e	4.86	15.00	4.10	32.20	0.139	21.39	2.1500 ± 0.0300	10.00 ± 1.00